



Experimental and Numerical Study on Thermal Performance of a Novel Direct Expansion Air-Source Heat Pump Heating System

Haobo Wang¹, Yuanda Cheng^{1*}, Dawei Wang¹, Weijin Peng¹, Zejian Ai¹, Jie Jia¹, Pengfei Duan¹ and Jinming Yang^{1,2}

¹College of Civil Engineering, Taiyuan University of Technology, Taiyuan, China, ²State Key Laboratory of Green Building in Western China, Xi'an University of Architecture and Technology, Xi'an, China

OPEN ACCESS

Edited by:

Libor Pekař,
Tomas Bata University in Zlín, Czechia

Reviewed by:

Wenzhe Wei,
Harbin Institute of Technology, China
Jiří Hejčík,
Brno University of Technology,
Czechia

*Correspondence:

Yuanda Cheng
chengyuanda@tyut.edu.cn

Specialty section:

This article was submitted to
Process and Energy Systems
Engineering,
a section of the journal
Frontiers in Energy Research

Received: 26 August 2021

Accepted: 22 December 2021

Published: 09 February 2022

Citation:

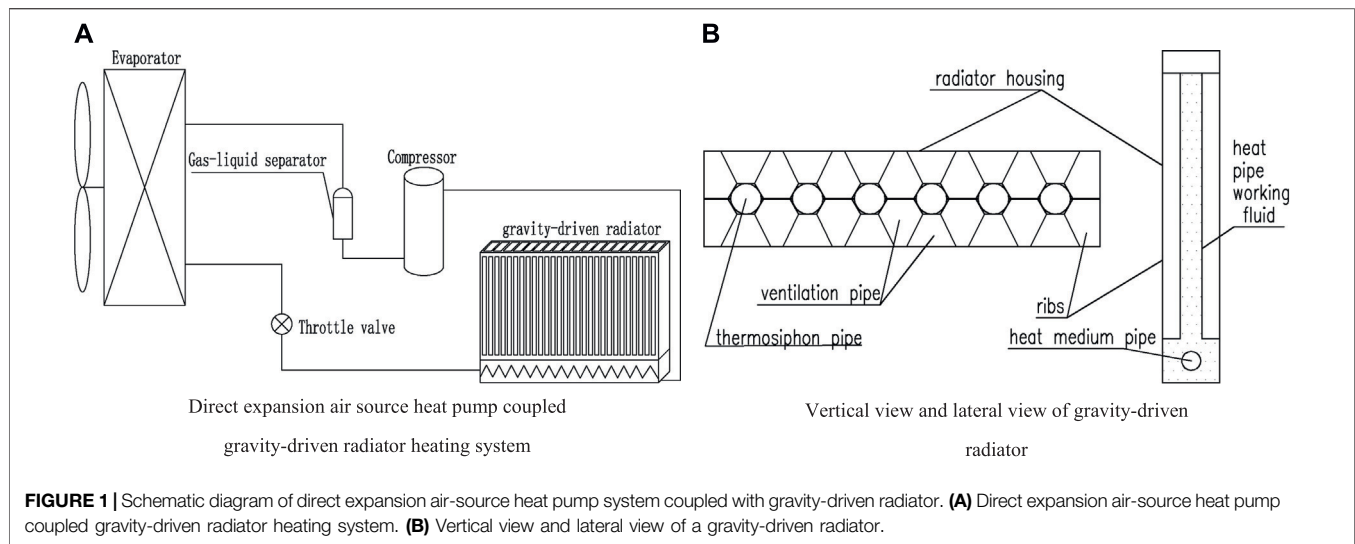
Wang H, Cheng Y, Wang D, Peng W,
Ai Z, Jia J, Duan P and Yang J (2022)
Experimental and Numerical Study on
Thermal Performance of a Novel Direct
Expansion Air-Source Heat Pump
Heating System.
Front. Energy Res. 9:765221.
doi: 10.3389/fenrg.2021.765221

In this paper, a novel direct expansion air-source heat pump heating system with a gravity-driven radiator as a heating terminal was developed, for the purpose of reducing the energy consumption and improving the thermal comfort of indoor personnel. The thermal response speed of the system at the start-up stage was experimentally studied firstly. The results showed that the thermal response speed of the developed system was slightly lower than that of a traditional air-source heat pump heating system with a convective heating terminal, but largely higher than that of an air-source heat pump floor radiant heating system. When the outdoor air temperature fluctuated between -5.2°C and -1.0°C , the average rising ratios of indoor air temperature at the start-up stage for the developed heating system and the traditional system are $10.8^{\circ}\text{C}/\text{h}$ and $13.8^{\circ}\text{C}/\text{h}$ respectively. On this basis, an optimization study was then conducted to further improve the thermal performance of the developed heating system. The numerical results indicated that integrating a cross-flow fan to the gravity-driven radiator is able to promote the thermal performance of the heating system obviously at the start-up stage, because the convection heat transfer of the radiator was highly enhanced. Among the simulation conditions, the time required for the air temperature at head height to reach the designed temperature is shortest when the flow angle of the fan is 0° with an air speed of 0.6 m/s . while setting the flow angle of the fan to -45° with an air speed of 0.4 m/s is recommended to achieve the most thermal comfort for the whole body.

Keywords: air-source heat pump heating system, gravity-driven radiator, thermal response speed, thermal comfort, radiation and convection coupled heat transfer

1 INTRODUCTION

The statistical data show that the energy used in building a heating system accounts for a large proportion of the whole building energy consumption. In 2018, urban heating energy consumption in northern China was as high as 212 million tec, accounting for 21% of the total building energy consumption in China (Building energy efficiency research center of Tsinghua University, 2020), which also led to a series of environmental pollution problems. Thus, air-source heat pump heating system has been widely used in the past few years in northern China because of its significant advantages in energy saving and environmental protection (Nishimura, 2002; Qu et al., 2012).



According to the different heating media used, the air-source heat pump system can be distinguished into two forms: indirect expansion and direct expansion. The former uses hot water to transfer heat to the room, while the latter transfers heat directly to the room through the refrigerant. Depending on the different heating terminal devices, the air-source heat pump system can also be distinguished into two types. One is the fan-coil heating terminal, in which the heat transfer is mainly dominated by convection. While the other one is the radiative heating terminal, including the traditional radiator and floor heating system, in which most of the heat is transferred by radiation. Researchers have conducted extensive research on air-source heat pump heating systems during the past decades, from the view point of energy efficiency, thermal comfort, etc. Previous studies revealed that the forced convection heat transfer has the advantage of fast response speed and strong ability to deal with heat load, but the thermal comfort of heating is relatively poor. By using air-source heat pump heating systems with a fan-coil heating terminal, excessive vertical temperature difference and draft feeling of human body often occurs because of the large air supply speed (Wang, 2002). In addition, hot air supplied from a high height of the room will also lead to an increase in temperature at the upper zone, and reduce the utilization rate of hot air energy in the occupied zone, which eventually results in the waste of energy (Li, 2010). In contrast, the radiation heat transfer is characterized by high comfort and good stability, but the response time of indoor air temperature rise is relatively long. Imanari's experimental result shows that radiant heating can improve thermal comfort by creating an environment with a small vertical temperature difference (Imanari et al., 1999). Through the research on the radiator heating system of air-source heat pump in an office building in Shanghai, Zhou found that the system can mitigate the human discomfort caused by cold radiation, but it is not suitable for intermittent heating due to the low indoor air temperature rise rate (Zhou et al., 2013). Through the comparison of the differences between various radiating end heating forms, Wang found that floor radiant

heating is not suitable for intermittent heating mode, and the intermittent heating performance of a radiator is better than that of floor radiant heating (Wang et al., 2018).

To overcome the shortcomings of the two heat transfer modes, and maximize their respective advantages, the optimization method of integrated coupling of the two heat transfer modes can be selected. At present, many related studies have been carried out on the combination of fan coil and floor radiation, wall radiation, or radiator (Jin et al., 2017; Zhao et al., 2017). To solve the above problems, this study performs an experimental analysis on the gravity-driven radiator, and to further accelerate the heat transfer speed of gravity-driven radiator, a new gravity-driven radiator based on the coupling heat transfer of radiant-convective is proposed.

2 EXPERIMENTAL STUDY

2.1 System Introduction

Different from the conventional air-source heat pump hot water heating system, the direct expansion air conditioning source heat pump uses liquid refrigerant as heat medium, which can effectively save the energy consumption due to the transportation of hot water. In the meantime, it can reduce the heat loss in the middle heat exchange process, and the operation of the system is shown in **Figure 1A**. The gravity-driven radiator proposed in this paper is a radiator heating terminal based on thermosyphon heat pipe technology, in which the working medium is alkyl dichloride and the size is $1,020\text{ mm} \times 80\text{ mm} \times 650\text{ mm}$ (Length \times Width \times Height). As shown in **Figure 1B**, the bottom of the gravity-driven radiator is equipped with a heat pump thermosyphon working medium heat exchanger that is connected with several thermosyphon tubes. In the evaporation zone at the bottom of the radiator, the thermosyphon working medium is heated and subjected to phase change by the high-temperature refrigerant (heat pump working medium) discharged by the heat pump compressor. The

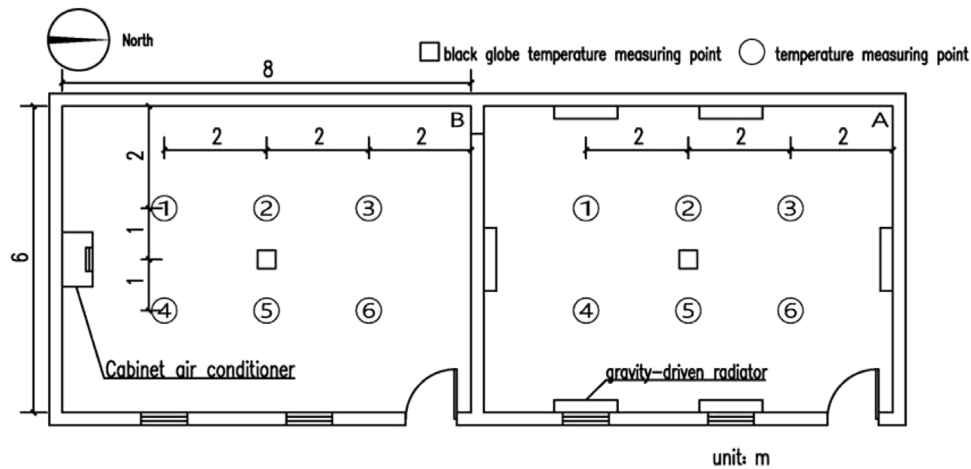


FIGURE 2 | Horizontal arrangement position of the experimental measuring points.

TABLE 1 | Measuring equipment, accuracy, and sampling frequency.

| Measurement item | Instrument | Accuracy | Recording frequency |
|-------------------------|--------------------------------|--------------------------------|---------------------|
| | | | (min/record) |
| Temperature | OMEGA-K-24 thermocouple | $\pm 0.1^{\circ}\text{C}$ | 1 |
| Humidity | HOBO humidity recorder | $\pm 0.1\%$, $\pm 2.5\%$ | 1 |
| Black globe temperature | AZ8778 black globe thermometer | $\pm 0.5^{\circ}\text{C}$ | 1 |
| Air speed | Testo hot-wire anemometer | $\pm 0.03\text{m/s} \pm 0.5\%$ | 5 |
| Wall temperature | Infrared thermometry | $\pm 0.5^{\circ}\text{C}$ | 20 |

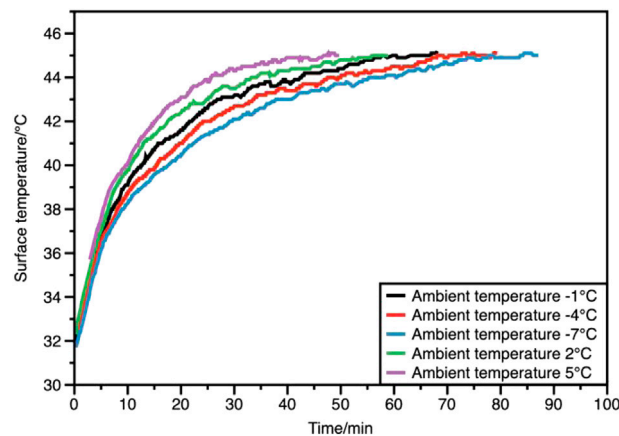
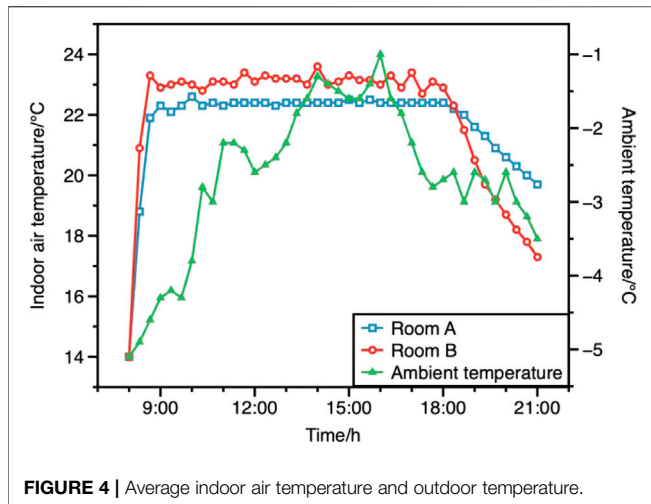


FIGURE 3 | Surface temperature of radiator.

gaseous working medium produced by boiling rises to the condensation zone, and heat is released through condensation at the pipe wall. The condensate then returns to the evaporation zone under the action of gravity, so as to complete a complete thermosiphon cycle. In addition, to enhance the heat dissipation performance of the radiator, fins are arranged on the outer wall of the pipe, thereby forming a closed ventilation channel.

2.2 Introduction to Experimental Platform

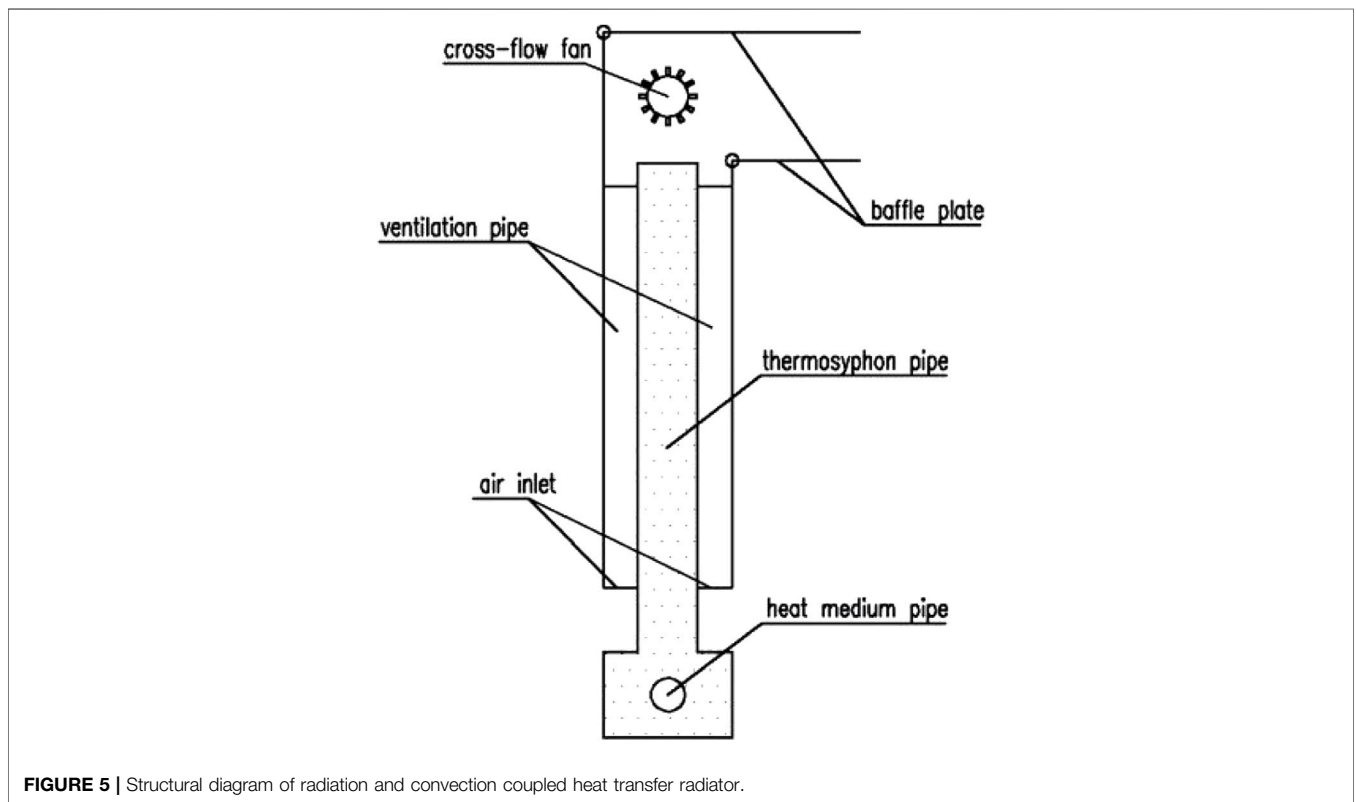
To study the response speed of the gravity-driven radiator of the air-source heat pump coupled gravity-driven radiator system during heating in winter, an experimental platform was established in an office building in Taiyuan, Shanxi Province of China. There are two office rooms with the same size and layout, namely, A and B; both rooms have

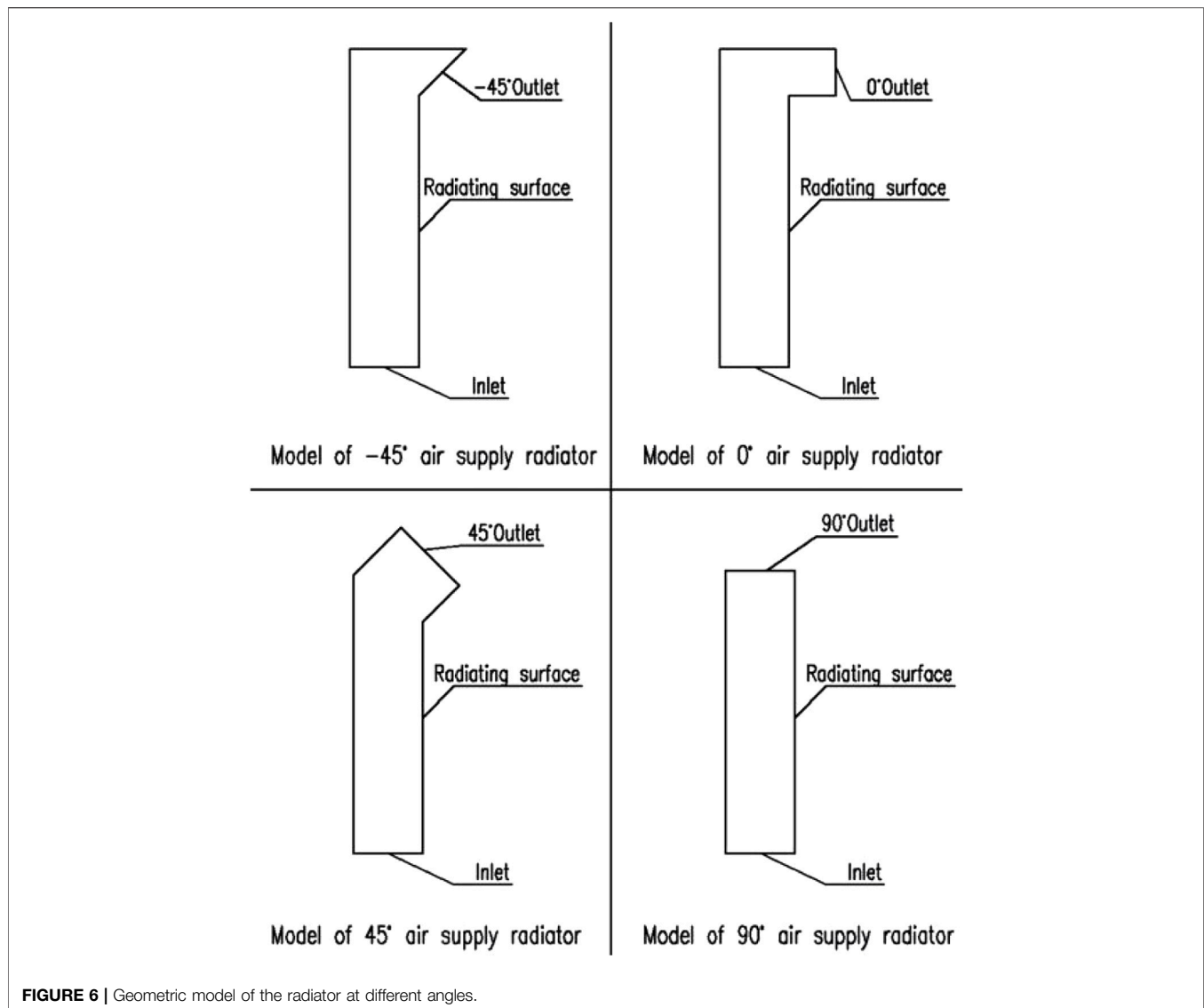


dimensions of $8\text{ m} \times 6\text{ m} \times 3\text{ m}$ (Length \times Width \times Height), and the heating area is 48 m^2 . The west wall of Room B is the external wall made of brick and concrete, with a thickness of about 300 mm, and there is no thermal insulation material on the outer layer. The rest of the walls are internal walls, which are made of bricks with a thickness of about 100 mm. The adjacent rooms are heating rooms, thereby ignoring the impact of heat transfer in the adjacent rooms. The air-source heat

pump with a rated power of 3.2 KW is used as the heat source in both rooms. The terminal of Room B adopts a traditional cabinet air conditioner, while Room A adopts a gravity-driven radiator. To meet the demand of room heating load, six gravity-driven radiators are arranged in Room A. The experimental test time was from January 18 to February 6, 2017 and from January 18 to February 7, 2018. The heating system was turned on at 8:00 and stopped at 18:00.

K-type thermocouples were used to measure the indoor air temperature. As shown in **Figure 2**, there are six measuring points arranged in horizontal direction in each room, with three heights of 0.1 m, 0.6 m and 1.1 m from the ground, respectively. The indoor air humidity and indoor black bulb temperature were recorded once per minute by using a HoBo humidity recorder and a black bulb thermometer, respectively, and the measurement points are located at the center of the room with a height of 1.1 m. The surface temperature of the radiator was measured at the center position of the radiator surface by using a K-type thermocouple. The inner surface of the enclosure was divided into six areas, and the temperature of the center point of each area was measured with a handheld infrared thermometer at a sampling interval of 20 min. The averaged value was taken as the surface temperature of surrounding walls. The indoor air flow rate measuring points were followed for the selection of the indoor air temperature measuring points, and the data were recorded every 20 min. The measuring instruments, accuracy, and sampling frequency are listed in **Table 1**.





3 EXPERIMENTAL RESULTS

3.1 Thermal Performance of the Gravity-Driven Radiator

The thermal performance of the gravity-driven radiator is one of the main factors influencing the thermal comfort of air-source heat pump heating systems. **Figure 3** presents the surface temperature variations of the gravity-driven radiator during the start-up stage, with different outdoor temperatures. It can be found that the stable surface temperature of the gravity-driven radiator is about 45°C , which satisfies the heating requirement. With different outdoor air temperatures, the time for the surface temperature of the radiator to stabilize is different. The higher the outdoor air temperature, the greater the surface temperature rising rate of the radiator, and the shorter the time for the radiator to enter the stable operation state. At the outdoor temperature of -7°C , -4°C , -1°C , 2°C and 5°C , the time taken for the radiator surface

temperature to reach stability is about 80, 70, 60, 50, and 40 min, respectively, and the corresponding surface temperature rising rates are $10.5^\circ\text{C}/\text{h}$, $12^\circ\text{C}/\text{h}$, $14^\circ\text{C}/\text{h}$, $16.8^\circ\text{C}/\text{h}$ and $21^\circ\text{C}/\text{h}$. The main reason is that the higher the outdoor air temperature, the higher the evaporation temperature of the heat pump, and the suction pressure of the compressor increases accordingly. Consequently, the refrigerant flow of the heat pump is also increased, so as to improve the heat input of the heat pump unit to the heat pump thermosyphon working medium heat exchanger. The temperature rise rate of the gravity-driven radiator increases accordingly. A previous study stated that in an air-source heat pump heating system with a floor heating terminal, the rising rates of floor surface temperature as well as indoor air temperature are relatively slow, because of the large thermal inertia of circulating water and radiant floor. The surface temperature rising rate of floor is about $1.3^\circ\text{C}/\text{h}$, when the outdoor temperature was 5°C (Wang and Tan, 2004). Thus, compared with the floor radiant heating, the thermal response speed of the gravity-

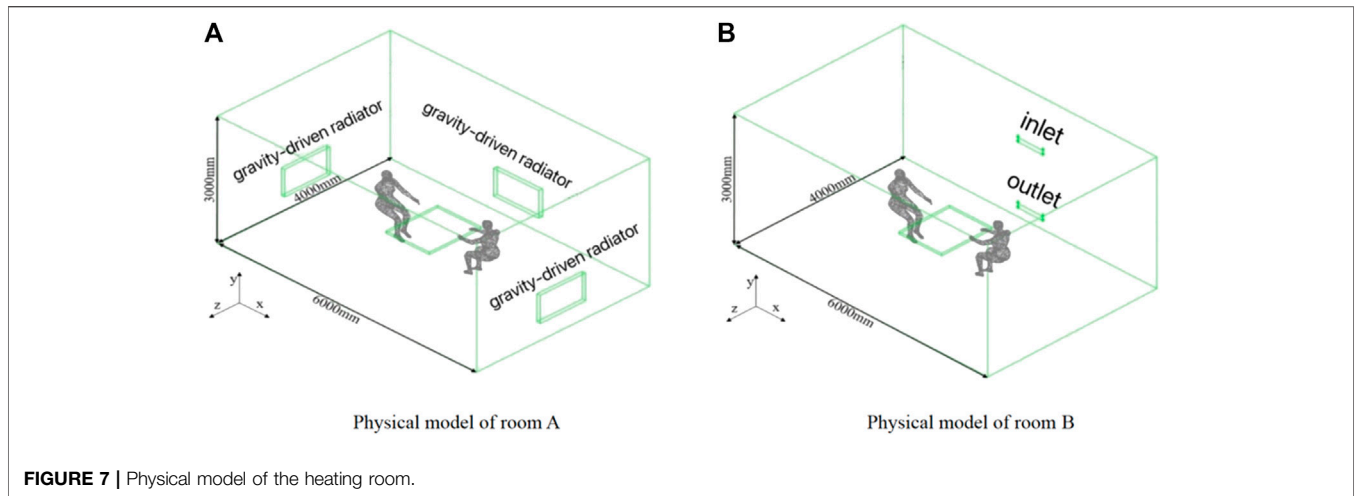


FIGURE 7 | Physical model of the heating room.

TABLE 2 | Related parameters of simulated working conditions.

| Working condition | Air supply angles | Air supply speed (m/s) |
|-------------------|-------------------|------------------------|
| 1 | | 0.2 |
| 2 | 90° | 0.4 |
| 3 | | 0.6 |
| 4 | | 0.2 |
| 5 | 45° | 0.4 |
| 6 | | 0.6 |
| 7 | | 0.2 |
| 8 | 0° | 0.4 |
| 9 | | 0.6 |
| 10 | | 0.2 |
| 11 | -45° | 0.4 |
| 12 | | 0.6 |

driven radiator is 15.2 times faster. Therefore, the gravity-driven radiator has the advantage of fast dynamic thermal response, and the users can quickly adjust the indoor temperature. In addition, the gravity-driven radiator is more suitable for intermittent operation to reduce heating energy consumption.

3.2 Indoor Air Temperature

Figure 4 compares the variations of indoor air temperature in Room A and Room B, from 08:00 to 21:00 during a typical day. It can be found that the indoor air temperature of both rooms are relatively stable within the range of 22–23.5°C, after a rapidly increasing at the start-up stage. As expected, the temperature rising speed in Room B with a traditional cabinet air conditioner is faster than that in Room A with a gravity-driven radiator, but the difference is not big. In Room B, the indoor air temperature reaches a basically stable state for about 40 min, and the average temperature rise rate of indoor air temperature is 13.8°C/h, while the values for Room A are 60 min and 10.8°C/h respectively. Previous studies revealed that under similar working conditions, the average indoor air temperature rise rate for the air-source heat pump floor radiant heating system is about 3.4°C/h (Wei et al., 2010), while that for the air-source heat pump auxiliary electric heating hot water radiator heating system is about 10.4°C/h (Cheng et al., 2018). Therefore, in air-source heat pump heating systems, using a gravity-driven radiator as a heating terminal will lead to a slightly lower indoor air temperature rising rate, compared with using a traditional cabinet air conditioner as a heating

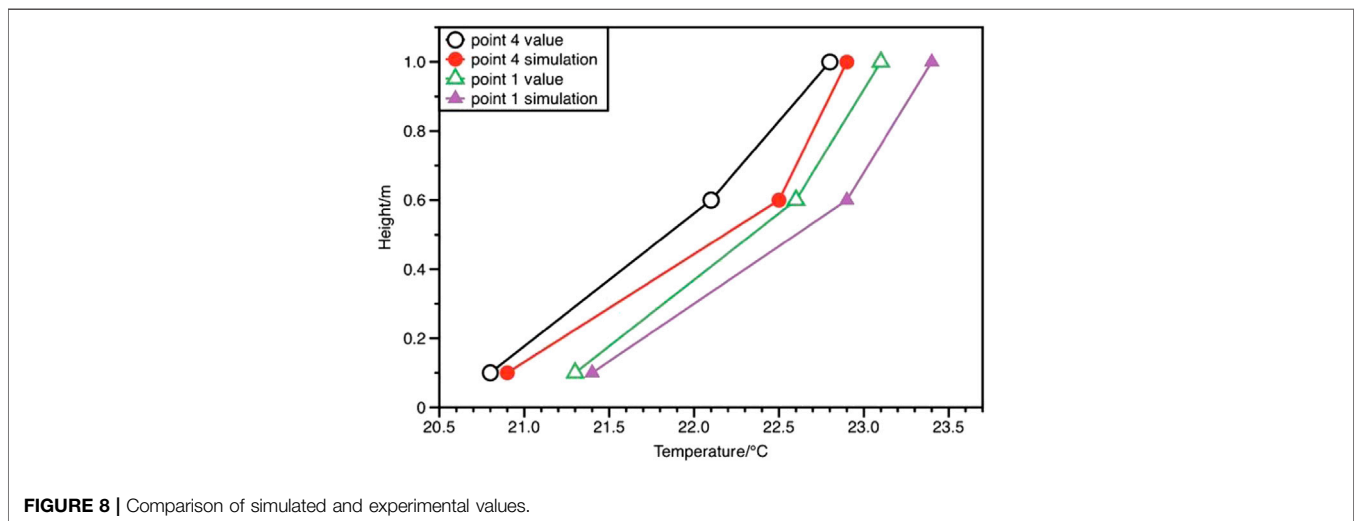


FIGURE 8 | Comparison of simulated and experimental values.

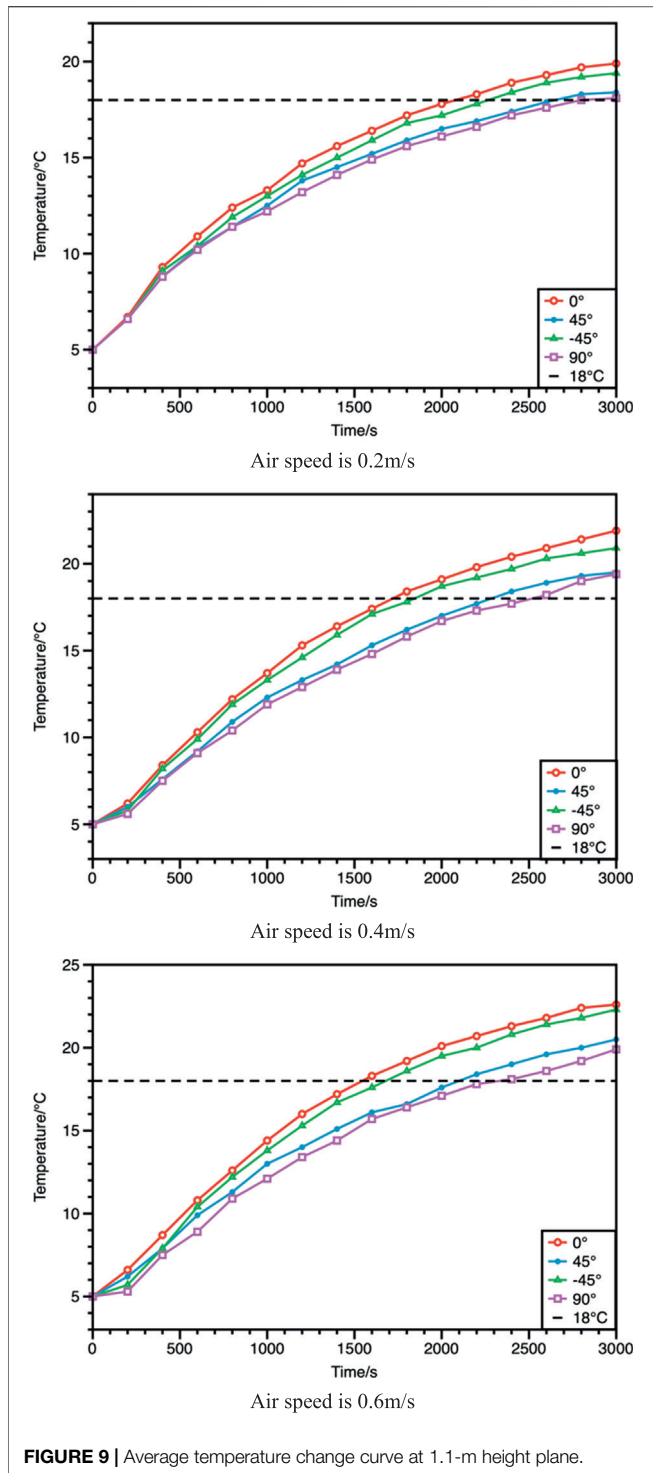


FIGURE 9 | Average temperature change curve at 1.1-m height plane.

terminal, but its thermal response performance is much better than using a floor heating terminal and has the potential of using the intermittent operation control strategy to save heating energy.

In the stable operation stage of the heating system, the indoor air temperature of Room A is maintained in the range of 22–22.6°C; while that in Room B is slightly higher than that in Room A, remaining in

the range of 22.5–23.4°C. However, the indoor air temperature is much more stable in Room A, compared with that in Room B. The indoor air temperature fluctuates frequently in Room B, and the maximum temperature difference is about 0.8°C. On the contrary, the change in indoor air temperature in Room A is relatively gentle.

It can also be found that the indoor air temperature decreasing rate in Room B is faster than that in Room A, when the heating systems are turned off. As shown in **Figure 4**, the indoor air temperature in Room B decreased from 22.9°C to 17.1°C within 3 h after the system shutdown, and the average temperature decreasing rate is 1.97°C/h. During the same period, the indoor air temperature in Room A decreased from 22.4°C to 19.6°C with an average temperature decreasing rate of 0.93°C/h. The main reason lies in the radiation heat exchange between the gravity-driven radiator and the room envelope in Room A. Since the building envelope itself has a certain heat storage capacity, the surface can still transfer heat to the room through radiation and convection, after shutting down the heating system. Thus, the air temperature dropping rate in Room A is much lower than that in Room B.

4 OPTIMIZATION RESEARCH

4.1 Introduction of Simulation Models and Cases

To further improve the response speed of the gravity-driven radiator and meet the demand of intermittent heating, **Figure 5** presents a new gravity-driven radiator with radiation and convection coupled heat transfer. Specifically, the air is sucked from the lower air outlet of the radiator by the crossflow fan, and discharged after being heated by the heat pipe wall in the ventilation channel; an adjustable deflector is equipped at the front end of the air supply outlet for the adjustment of the air supply angle; **Figure 6** illustrates the geometric model of the radiator at different angles.

In this research, the authors optimize the gravity-driven radiator by CFD. Geometric modeling has to meet the requirements of geometric similarity, physical similarity, and condition similarity to get the results close to the real situation. This simulation makes a reasonable simplified calculation of the model. The length of the room is only half of the actual length, and the space dimensions of different heating systems are 4 m × 6 m × 3 m (Length × Width × Height), and the dimensions of the gravity-driven radiator are 1,050 mm × 80 mm × 650 mm (Length × Width × Height). According to the actual position of the cabinet-type air conditioner, the air supply outlet and the air return outlet at the end of the hot air conditioner are arranged on the same side, and the dimensions are 600 mm × 100 mm (Length × Width). The inlet is used as a velocity inlet with an air speed of 2 m/s and the temperature of 35°C, and the outlet is set as free outflow. Each room has two sitting mannequins, one is at each end of a rectangular desk, and the other is 1,200 mm × 1,000 mm × 50 mm (Length × Width × Height). The physical model is shown in **Figure 7**.

Considering the air supply speed on the thermal comfort will also have an impact; after verifying the reliability of the model, this paper studies the indoor air temperature response speed and thermal comfort of the new gravity-driven radiator with the air-source heat pump heating system under different air supply

TABLE 3 | Thermal comfort evaluation at different air supply angles and air speeds.

| Angle | Air speed | Height (m) | | | | | | | | |
|-------|-----------|------------|---------|------|-------|---------|-------|-------|---------|-------|
| | | 0.1 | | | 0.6 | | | 1.1 | | |
| | (m_s) | PMV | PDD (%) | DR | PMV | PDD (%) | DR | PMV | PDD (%) | DR |
| 90° | 0.2 | -0.64 | 13 | 0 | -0.6 | 12 | 0 | -0.58 | 12 | 3.5% |
| | 0.4 | -0.74 | 16 | 0 | -0.72 | 16 | 4.4% | -0.58 | 12 | 4.5% |
| | 0.6 | -0.74 | 16 | 0 | -0.66 | 14 | 5.2% | -0.49 | 10 | 6.1% |
| 45° | 0.2 | -0.66 | 14 | 0 | -0.66 | 14 | 0 | -0.62 | 13 | 4.1% |
| | 0.4 | -0.72 | 16 | 0 | -0.64 | 13 | 4.3% | -0.49 | 10 | 4.8% |
| | 0.6 | -0.72 | 16 | 3.1% | -0.64 | 13 | 5.7% | -0.47 | 10 | 7.9% |
| 0° | 0.2 | -0.62 | 13 | 0 | -0.58 | 12 | 0 | -0.51 | 11 | 6.8% |
| | 0.4 | -0.64 | 14 | 0 | -0.6 | 13 | 7.2% | -0.46 | 9 | 10.1% |
| | 0.6 | -0.66 | 14 | 2.9% | -0.62 | 13 | 13.6% | -0.46 | 9 | 16.3% |
| -45° | 0.2 | -0.58 | 12 | 2.7% | -0.54 | 11 | 4.4% | -0.48 | 10 | 5.7% |
| | 0.4 | -0.49 | 10 | 3.2% | -0.48 | 10 | 8.8% | -0.44 | 9 | 12.1% |
| | 0.6 | -0.49 | 10 | 8.8% | -0.49 | 9 | 11.6% | -0.53 | 11 | 17.5% |

angles and air supply speeds; a total of 12 working conditions are simulated in this study, as shown in **Table 2**.

4.2 Simulation Model Validation

The physical model is consistent with the experimental platform, and the simulation results are compared with the measured data at 14:00 on a typical day. The root mean square error (RMSE) is selected as the evaluation index. The comparison between the simulated and experimental values of the air temperature distribution at the vertical height of indoor air temperature measuring Point one and measuring Point four is shown in **Figure 8**, which shows that the maximum temperature difference between the simulated and measured air temperature values is no more than 1°C, and the root mean square error is 21%. In the case that the RMSE value is less than 30%, which can be applied to further simulate research within an acceptable range, the model can be considered to be reliable.

4.3 Simulation Results

Since the thermal sensation of the head greatly influences the overall thermal sensation of the human body (Duanmu, 2007), the 1.1-m height plane, which is the height of the head at the sitting position (hereinafter referred to as the 1.1-m height plane), will be used as the main standard for the comparison of response time and thermal comfort under different optimization schemes. **Figure 9** illustrates the average temperature change curve of the 1.1-m height plane under different air angles and air supply speeds. As can be seen from the figure, when the new gravity-driven radiator is working, as shown in **Figure 5**, the indoor air temperature rises rapidly, and the air temperature rise rate tends to be flat after heating for a certain time. GB/T5 0785-2012 stipulates that the standard for Class II comfort of thermal environment of heating is as follows: the air speed is not lower than 0.2 m/s, and the ambient temperature is within the range of 18°C–22°C (GB/T5 0785-2012, 2012). The differences in air supply angle and speed have an impact on the time required for the average temperature of the 1.1-m height plane to reach the minimum required temperature of 18°C (hereinafter referred to as the required time).

4.3.1 Indoor Air Temperature Response Time

The indoor air temperature changes with time under different air supply speeds and different air supply angles, as shown in **Figure 9**. It

can be seen from **Figures 1–9** that at the air speed of 0.2 m/s and the air supply angle of -45°, when the required temperature for thermal comfort is 18°C, indoor air temperature rise is about 20.5°C/h; when the air supply angle is 0°, it meets the requirements of thermal comfort, and the temperature rise is about 22.4°C/h; in the case that the air supply angle is 45°, the temperature rise is about 17.9°C/h, temperature rise is required to make the average temperature of the plane at the height of 1.1 m reach 18°C, while when the air supply angle reaches 90°, the temperature rise is about 16.7°C/h, thereby meeting the temperature required for thermal comfort. It is explored that at the air speed of 0.2 m/s, the time required for the air supply angle at 18°C is the shortest. When the air speed is 0.4 m/s, the air supply angle changes from -45° to 90° to meet the required temperature of thermal comfort, and the temperature increases are about 25.6°C/h, 27.4°C/h, 20.5°C/h and 18.6°C/h respectively. In addition, the air supply temperature is 0.6 m/s, When the air supply angle changes from small to large, the temperature rise changes are about 27.7°C/h, 30.8°C/h, 22.3°C/h and 19.5°C/h respectively, meeting the temperature requirements of thermal comfort.

It can be found that when the air supply speed remains unchanged, with the air supply angle decreasing from 90° to -45°, the required time decreases and then increases, which is due to the fact that the initial reduction of the air supply angle is conducive to enhancing the convective heat transfer effect between the hot air and the air at the height of the human head while sitting, and the required time decreases accordingly. However, in the case that the air supply angle decreases to -45°, the hot air blown out of the tuyere first heats the air below the human head and then floats up depending on the density difference before heat exchange with the air above. Therefore, when the average temperature of the 1.1 m height plane is taken as the comparison standard, the time required for -45° air supply is higher than 0°. When the air supply angle is 0°, the time required is the shortest, and the time needed to reach the required temperature of thermal comfort under different air supply speeds is compared. It is found that the greater the air supply speed, the shorter the time required to reach 18°C. When the air speed increases from 0.2 m/s to 0.6 m/s, the difference between the time required for 0° air supply and that for -45° air supply increases gradually as well. The reason is that at the air supply angle of -45°, the increase of the air supply speed can effectively inhibit the floating of hot air. Most of the heat is used to

heat up the air below the 1.1-m height plane, and the rising rate of air temperature at the 1.1-m height plane becomes relatively gentle. Based on the comparison of the above 12 simulation conditions, at the air supply angle of 0° and the air supply speed of 0.6 m/s , the maximum temperature rise meeting the temperature requirements of thermal comfort is about $30.8^\circ\text{C}/h$. When the air supply angle remains unchanged, the increase in air supply speed can greatly reduce the required time, and the reduction range of the required time decreases gradually with the increase in air supply speed.

4.3.2 Thermal Comfort Performance

Because the thermal environment at the terminal of the gravity-driven radiator is relatively even, there is no obvious air temperature stratification, and the layout position of radiators in the room is uniform and symmetrical. Moreover, the effects of radiation asymmetry and air speed asymmetry can almost be ignored, and the thermal environment using the gravity-driven radiator can be regarded as an ideal uniform environment. Therefore, when further analyzing the thermal comfort of indoor environment under different air supply angles and air speeds, according to the provisions of ISO7730 (International Standard, 1984), the PMV, PDD, and DR (blowing feeling index) will be taken as the evaluation indexes. The indoor Level II thermal comfort environment requires that PMV be -0.5 – 0.5 , PDD $< 10\%$, and DR $< 20\%$. This paper studies the sitting posture of the human body; therefore, the three indoor height planes of 0.1 m (ankle), 0.6 m (abdomen), and 1.1 m (head) are selected for comparative analysis. Besides, all PMV, PDD, and DR evaluation values refer to the average values on the height plane.

The thermal comfort evaluation results of indoor environment under different air supply angles and air supply speeds are shown in **Table 3**. As seen from **Table 3**, although the changes in air supply angle and air speed have an impact on the DR of 0.1 m (ankle), 0.6 m (abdomen), and 1.1 m (head), under all simulated working conditions, the average blowing sensation index (DR) increases with the increase in height from the ground at the same angle and air supply speed; in the case that the air supply angle is constant, the DR increases with the increase in air supply speed. When the air supply angle is -45° and the air supply speed is 0.6 m/s , the average blowing sensitivity index value is the highest, and the value at a height of 1.1 m from the ground is 17.5% . It can be found that the average blowing sensation index under all simulated working conditions is no more than 20% , indicating that the blowing sensation of air flow on human body is within an acceptable range. When the air supply angle and air supply speed are constant, the PMV decreases with the increase of the height from the ground; at constant air supply speed and reduced air supply angle, the thermal comfort evaluation of each height shows an upward trend; **Table 3** shows that at an air supply angle of -45° and an air speed of 0.4 m/s , the simulated average values of PMV and PDD at the ankle of 0.1 m are -0.49 and 10% , respectively, while those at the abdomen of 0.6 m are -0.48 and 10% , and those at the height of 1.1 m above the ground (about the head) are -0.44 and 9% , respectively. Therefore, the thermal comfort of the human body is within the requirements of Class II thermal comfort environment. The thermal environment under this heating condition is available for high crowd satisfaction. When the air speed is further increased, the dissatisfaction rate

PDD value of the population of 0.6 m (abdomen) and 1.1 m (head) increases instead, and the PMV value also exceeds that required for thermal comfort, indicating that the increase in air speed at this time is not beneficial to the improvement of thermal comfort, or even bring the risk of reducing thermal comfort.

5 CONCLUSION

- 1) It is experimentally found that during the gravity-driven system start-up stage, the average indoor air temperature rise rate of $10.8^\circ\text{C}/h$ is slightly lower than that of $13.8^\circ\text{C}/h$ at the heating terminal of air conditioning. However, compared with other air-source heat pump radiant heating systems, it can quickly improve the indoor temperature. The gravity-driven radiator is characterized by fast start-up temperature rise and better dynamic response than the floor radiation system, which is suitable for intermittent operation mode to save heating energy consumption.
- 2) In this paper, a convection and radiation coupled gravity-driven radiator was proposed. By installing a cross-flow fan, the radiation and convection coupled heat transfer can be realized at the gravity-driven radiator, thereby significantly speeding up the response speed of indoor temperature during heating. The simulation study found that the increase in air supply speed can greatly reduce the required time, and the reduction range of the required time decreases gradually with the increase in air supply speed when the air supply angle remains unchanged.
- 3) Without affecting thermal comfort, the new gravity-driven radiator can be optimized with an air supply angle of -45° and the air supply speed is limited to 0.4 m/s , the PMV is within the range of -0.5 – 0.5 , the PDD is less than 10% , and the DR is less than 20% , indicating that the thermal environment can be comfortable to all parts of the human body at this time.

DATA AVAILABILITY STATEMENT

The original contributions presented in the study are included in the article/supplementary material. Further inquiries can be directed to the corresponding author.

AUTHOR CONTRIBUTIONS

HW was in charge of experimental results analysis and the writing of the paper; DW contributed to the data analysis; YC was in charge of the whole research; JJ, ZA, WP and JY participated in the experimental work; YC and PD contributed to the revision of the paper.

ACKNOWLEDGMENTS

The authors appreciate the financial supports from the National Key Research and Development Program of China (No. 2018YFD1100701-05), the National Natural Science Foundation of China (No. 51808372), Key Research and

Development (R and D) Projects of Shanxi Province (Nos. 201903D321043 and 201903D121037), the Open Foundation Program of State Key Laboratory of Green Building in

Western China (No. LSKF202011), and the Postgraduate Innovation Project of Shanxi Education Department (No. 2021Y235).

REFERENCES

- Building energy efficiency research center of Tsinghua University (2020). Annual Report on China Building Energy Efficiency [R] (In Chinese). Beijing, China: China Architecture & Building Press 2020 (4).
- Cheng, H., Nian, M., Wang, G., Tang, G., and Zhang, J. (2018). Measurement and Analysis of Temperature Intermittent Heating in Hefei Area[J]. *Building energy efficiency* 46 (8), 108–112. doi:10.3969/j.issn.1673-7237.2018.08.021
- Duanmu, L. (2007). *The Study on thermal Environment and comfort for Desktop-Based Task-Ambient Air conditioning[D]*. Dalian, China: Dalian University of Technology.
- GB/T5 0785-2012 (2012). *Evaluation Standard for Indoor thermal Environment in Civil buildings[S]*. Beijing: China Architecture & Building Press.
- Imanari, T., Omori, T., and Bogaki, K. (1999). Thermal comfort and Energy Consumption of the Radiant Ceiling Panel System. Comparison with the Conventional All-Airsystem. *Energy Build* 30 (2), 167–175. doi:10.1016/s0378-7788(98)00084-x
- ISO. International Standard (1984). *Moderate thermal Environments-Determination of the PMV and PPD Indices and Specification of Conditions for thermal comfort*. Geneva: International Standards Organization.
- Jin, H., Zhang, Y., and Wu, Q. (2017). A Coupled Air-Conditioning System of Radiation and Convection Comparative Analysis of Indoor Environment [J]. *Building Energy Environ.* 6, 25–29. doi:10.3969/j.issn.1003-0344.2017.06.006
- Li, N. (2010). *Building Environment[M]*. Beijing: Chemical Industry Press.
- Nishimura, T. (2002). Heat Pumps-Status and Trends” in Asia and the Pacific [J]. *Int. J. Refrigeration* 25 (4), 405–413. doi:10.1016/s0140-7007(01)00031-7
- Qu, M., Xia, L., Deng, S., and Jiang, Y. (2012). An Experimental Investigation on Reverse-Cycle Defrosting Performance for an Air Source Heat Pump Using an Electronic Expansion Valve. *Appl. Energy* 97, 327–333. doi:10.1016/j.apenergy.2011.11.057
- Wang, E., and Tan, H. (2004). Application Study on Floor Heating System with Air Source Heat Pump in Shanghai Area[J]. *Building Energy Environ.* 06, 25–29.
- Wang, Y. (2002). Measurement and Analysis of thermal Environment of Heated and Heat Pump Air-Conditioned Rooms[J]. *J. HV&AC* 32 (3), 18–19. doi:10.3969/j.issn.1002-8501.2002.03.006
- Wang, Z., Luo, M., Geng, Y., Lin, B., and Zhu, Y. (2018). A Model to Compare Convective and Radiant Heating Systems for Intermittent Space Heating. *Appl. Energy* 215, 211–226. doi:10.1016/j.apenergy.2018.01.088
- Wei, X., Zeng, Z., Lu, J., Wu, J., and Wei, Z. (2010). Experiment Study on Direct Floor Radiant Heating System of Air Source Heat Pump[J]. *J. HV&AC* 40 (7), 103–107. doi:10.3969/j.issn.1002-8501.2010.07.026
- Zhao, Q., Wang, J., Feng, X., and Li, J. (2017). Influencing Factors Analysis on Cooling Capacity of Fan Coil Unit and Radiant Floor Combined System[J]. *Refrigeration And Air-Conditioning* 6, 19–23.
- Zhou, B., Tan, H., Wang, L., Chen, S., and Zhuang, Z. (2013). Application Study on Radiator Heating System with Air-Source Heat Pump in Shanghai Area[J]. *J. HV&AC* 43 (9), 83–86. Available at <https://d.wanfangdata.com.cn/periodical/ChlQZXJpb2RpY2FsQ0hJTmV3UzIwMjExMjMwEg1udGt0MjAxMzA5MDE3GghwNDQ5eG85eg%3D%3D>.

Conflict of Interest: The authors declare that the research was conducted in the absence of any commercial or financial relationships that could be construed as a potential conflict of interest.

Publisher’s Note: All claims expressed in this article are solely those of the authors and do not necessarily represent those of their affiliated organizations, or those of the publisher, the editors, and the reviewers. Any product that may be evaluated in this article, or claim that may be made by its manufacturer, is not guaranteed or endorsed by the publisher.

Copyright © 2022 Wang, Cheng, Wang, Peng, Ai, Jia, Duan and Yang. This is an open-access article distributed under the terms of the Creative Commons Attribution License (CC BY). The use, distribution or reproduction in other forums is permitted, provided the original author(s) and the copyright owner(s) are credited and that the original publication in this journal is cited, in accordance with accepted academic practice. No use, distribution or reproduction is permitted which does not comply with these terms.